REVIEWER-1

This paper proposes using surface current maps derived from High Frequency Radars (HFR) to define a Coastal Upwelling Index (CUI), a quantity that is usually obtained from other met-ocean parameters such as wind speed, sea level pressure field or Sea Surface Temperature (SST). The advantage of the HFR-derived CUI (CUI-HFR) over classical indices is the ability to provide spatial maps (instead of mere time series) and to account for the ocean circulation which cannot be apprehended by the other parameters. To assess the relevance of this new index, the data originating from 2 networks of HFR in the North-West Iberian Peninsula are processed and compared with the traditional wind-derived CUI (CUI-WIND) as well as with a CUI defined from a global operational 3D ocean model (CUI-GLOBAL). In addition, some satellite measurements of SST and Chlorophyll are used to corroborate the upwelling/downwelling events.

The paper is interesting, well written and well documented. It introduces a promising and important new application of HFR. For these reasons I think it deserves acceptance for publication. I have only a list of minor remarks and questions, whose clarification could help consolidate the methodology and results. I list them below in order of appearance in the text.

Many thanks to Dr. Guèrin for the detailed review and the number of useful tips provided. Please find below a thorough point-by-point response with the hope of improving the quality of the document to make it acceptable for final publication.

1) Section 4, page 7: ocean-based CUI and wind-based CUI are found strongly correlated. Does this merely mirror the correlation between winds and surface currents or is there a deeper reason?

Yes, indeed the wind-surface current linear correlation is one of the premises for computing the constant parameter of the CUI (as exposed in section 3, page 6), which assume that the alongshore wind stress is the primary driver of upwelling circulation and that HF radar-derived surface currents are highly responsive to local wind (e.g. Paduan and Rosenfeld, 1996).

Nevermind, it is worth clarifying that in equation [1] of this manuscript (page 6) the wind velocity components (u and v) are measured at one single point (Silleiro buoy location, 9.43ºW, 42.12ºN) and used here as a proxy for the local open sea wind conditions. By contrast, in equation [3], the HFR-derived surface current velocities (u and v) are measured over a selected subregion (the yellow area in Annex 1-a) and then spatially averaged.

Reference:

Paduan, J. D., and Rosenfeld, L. K. (1996), Remotely sensed surface currents in Monterey Bay from shore-based HF radar (Coastal Ocean Dynamics Application Radar), J. Geophys. Res., 101(C9), 20669– 20686, doi:10.1029/96JC01663.

What would be the correlation coefficient between the components of wind and current velocities (u-wind versus u-current and v-wind versus v-current)?

Please find below the hourly timeseries (for the concurrent period 1 August - 31 December 2021) and the correlation coefficient derived from the best linear fit of scatter plot, not only for the zonal (u) and meridional (v) velocities but also for the total velocity. As explained later in this document, a 25-h running-mean filter was applied to the wind and current velocities.

As it can be observed below, the zonal component is just moderately correlated (0.43), whereas the meridional component appears to be highly correlated (0.80) for the 5-month period. This confirms our previous statement: the alongshore wind (v) stress is the primary driver of upwelling circulation in the NWI area. Finally, the total wind speed observed at Silleiro buoy and the HFR-derived total current velocity (averaged over the aforementioned subregion) are also significantly correlated, with a correlation coefficient of 0.71.

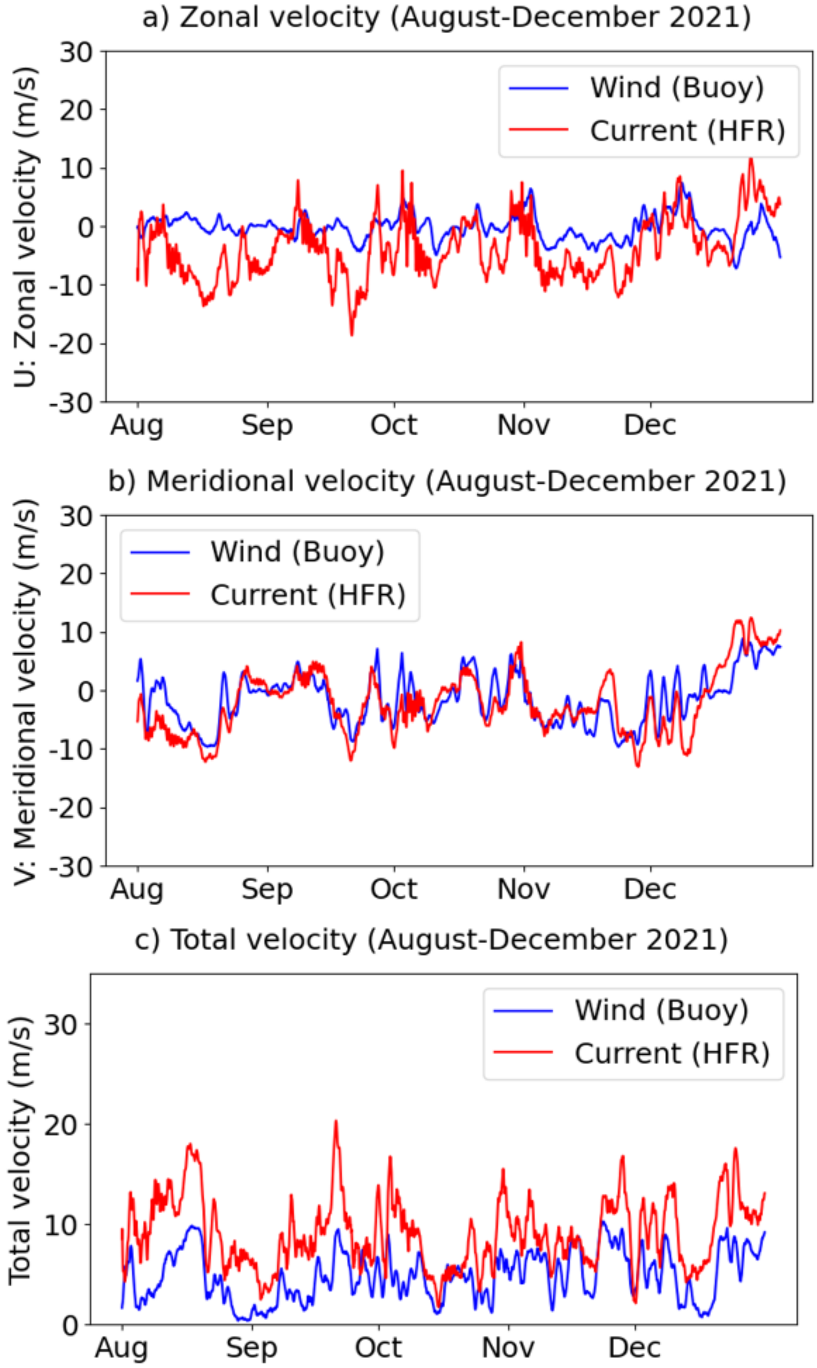

$U_{current}$ multiplied by 97.2 to get a slope=1.0 and:
Correlation = 0.43
Intercept = -3.61

$V_{current}$ multiplied by 59.2 to get a slope=1.0 and:
Correlation = 0.80
Intercept = -0.55

$speed_{current}$ multiplied by 72.5 to get a slope=1.0 and:
Correlation = 0.71
Intercept = 4.26

2) I see no statistical comparison (correlation coefficient, RMS difference) to compare CUI-GLOBAL and CUI-HFR. This would be interesting to see how close they are in order to coarsely quantify the accuracy that can be expected from these two types of estimators.

We fully agree that the statistical comparison between CUI-GLOBAL and CUI-HFR could be beneficial, so we have complemented the Annex-2 figure by adding a new panel d). In this new panel (shown below), the best linear fit of the scatterplot for a 5-month period (August-December 2021) and the associated metrics show the significant agreement between both estimators, as reflected by a correlation coefficient of 0.91 and a slope (0.96) rather close to 1.

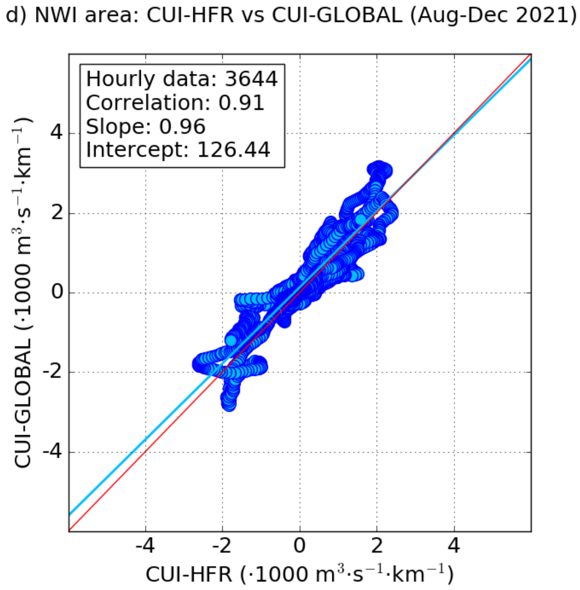

Additionally, we have moved panel e) of Annex-2 figure to a new figure (Annex-3, focused on 2020 year), which has also been complemented with the related scatterplot and metrics, highlighting again the potential of CUI-GLOBAL as a proxy of upwelling conditions in the study area.

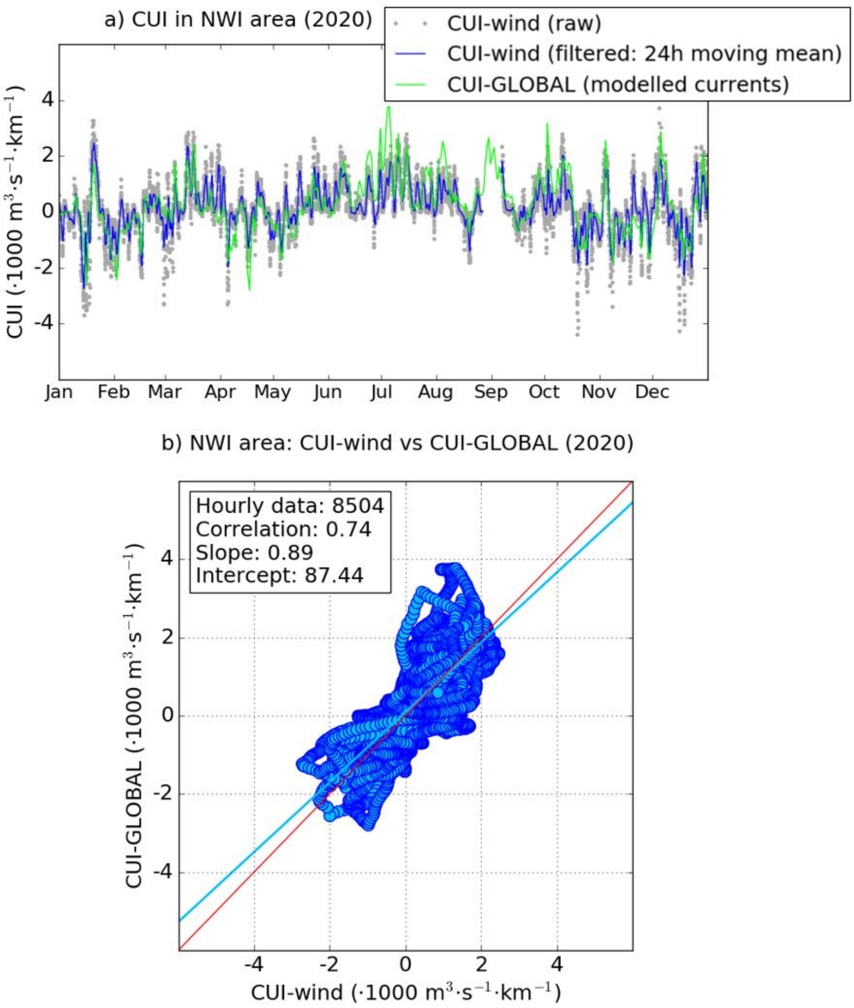

Annex 3: a) Time Series of two hourly Coastal Upwelling Index (CUI) in the North-Western Iberia (NWI) region (a) for the entire 2020 as derived from wind observations from Silleiro Buoy (CUI-WIND) and from modelled surface currents (CUI-GLOBAL). CUI-WIND raw (grey dots) was filtered by applying a 25-h moving mean (blue line). b) Best linear fit of scatter plots between CUI-GLOBAL and CUI-WIND (filtered) in NWI area for the entire 2020.

3) What is the influence of tidal currents on the hourly CUI-HFR? As the CUI-GLOBAL is free of tide, I suppose this induces an extra difference?

Running-mean filters are the simplest low-pass filters to apply to ocean observations with the aim of: i) visually smoothing the time-series graph; and ii) revealing an outline of longer-period variations (Shirakata et al., 2016). Within this context, and considering the semi-diurnal nature of the tide in the area of study, most of the tidal signal was filtered out as HFR current hourly data fields were averaged over 25-h hours to remove the main diurnal and semidiurnal tidal constituents, particularly the M2 signal, which is the largest harmonic constituent in the study area. Shorter digital filters (like the one used in this work) are generally preferred because they can yield a longer output time series from a practical finite input time series with less loss of length at both ends of the input series.

Although the 25-h running-mean filter leaves fortnightly, monthly, semi-annual tidal components (e.g. M_f, M_m, S_{sa}, etc.), they are considered to play a marginal role in the differences detected between CUI-HFR and CUI-GLOBAL. On the contrary, the discrepancies between both CUIs are supposed to be attributable to a major extent to the intrinsic limitations of the global ocean model and the uncertainties in the HFR derived current measurements.

To better clarify this point, a sentence has been added to the manuscript, in particular, in section 3 ("Methodology").

Reference:

Shirahata, K., Yoshimoto, S., Tsuchihara, T. and Ishida, S. Digital Filters to Eliminate or Separate Tidal Components in Groundwater Observation Time-Series Data. Japan Agricultural Research Quarterly (JARQ), 2016, Vol. 50, Issue 3, 241-252, doi:10.6090/jarq.50.241.

4) page 8 line 228: The «overall concordance» between HFR-CUI and GLOBAL-CUI seems somewhat euphemistic when looking at Figure 3. There are some important differences both in magnitude and direction of the currents. Is there any clue as to which data (HFR or model) is more reliable?

We agree with the reviewer that the surface circulation maps present some differences that must be further discussed along with their source (e.g. limitations of the global model at coastal scales, littoral processes misrepresented, etc.).

However, our main intention was to indicate that, despite those discrepancies in magnitude and direction, both the HFR-derived and GLOBAL-derived maps in Figure 3 share some common features at synoptic scale, namely: i) the prevailing S-SW surface flow, as response to northerly winds during UPW episodes, ii) the general poleward flow (the so-called Iberian Poleward Current) along the NW Iberian shelf during DOW episodes (Figure 3, e-f). Furthermore, both types of maps present rather uniform, smooth patterns where no submesoscale structures (i.e. eddies, small meanders, vortexes, etc.) are evidenced since the wind-induced homogenization also reduced the patchiness.

To avoid any misunderstanding, we have rephrased the aforementioned sentence.

With regards to the question about the reliability of HFR estimations and GLOBAL model outputs, it has been broadly accepted that quality-controlled HFR estimations should act as "ground truth". To support this assumption, a wide variety of previous works can be found in the literature where ocean forecasting models were assessed against HFR-derived surface currents, used as consistent benchmark reference to compare with (Berta et al., 2014, Lorente et al., 2021; Aguiar et al., 2020; Sotillo et al., 2021, to name a few).

Finally, we would like to provide a flavor of the basic functionalities of the NARVAL (North Atlantic Regional VALidation) software package (Lorente et al., 2019) in order to elucidate the accuracy of the GLOBAL forecast model against the Galician HFR on a monthly basis (August 2021). The figure below shows in the pop panel (from left to right): a) Monthly averaged HFR derived surface currents; b) Monthly averaged GLOBAL forecast model surface currents; c) Correlation of zonal and d) meridional surface currents between the GLOBAL forecast model and the HFR. In the bottom panel (from left to right): a) RMSE of zonal and b) meridional surface currents; c) Magnitude of the complex correlation (i.e. index) and d) phase between HFR and GLOBAL model-predicted currents.

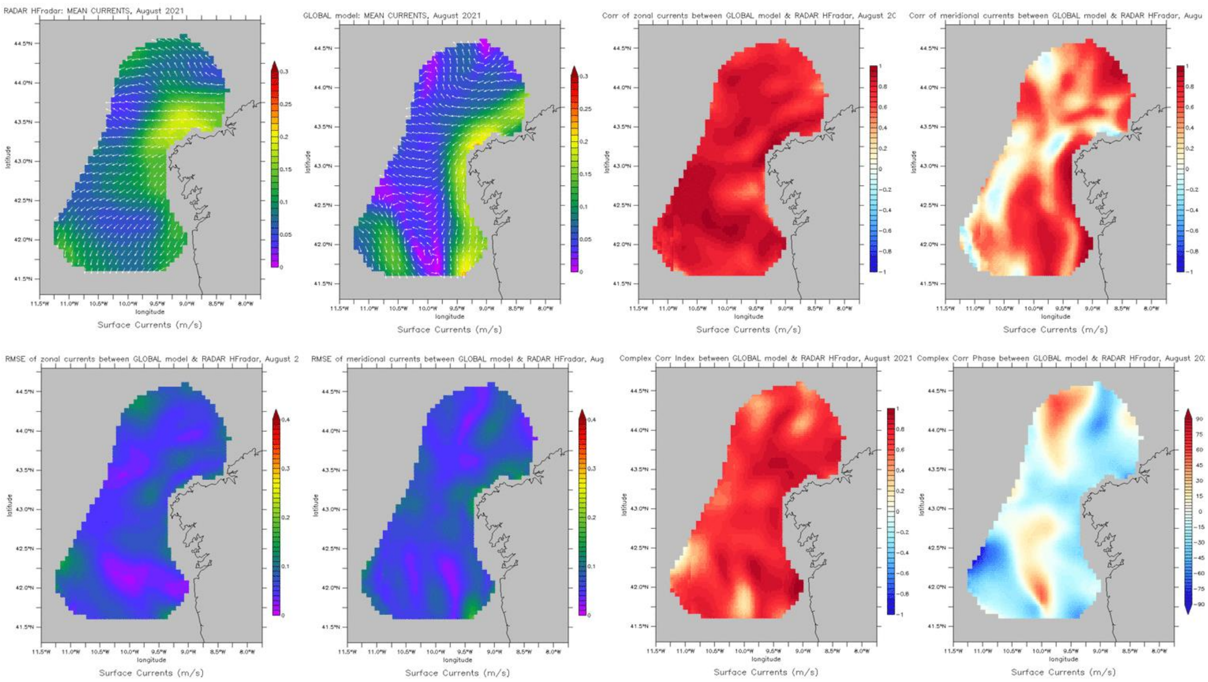

As it can be seen above, the degree of concordance in coastal areas is good (particularly for the zonal component and for the complex correlation coefficients, which are both above 0.7) and moderate RMSE values (higher for the meridional component in the near-coastal areas). It is also true that the veering angle (between HFR current vectors and GLOBAL current vectors) ranges from -15º to -30º on average, indicating thereby the counter-clockwise rotation of GLOBAL vectors with respect to HFR vectors. In other words, while HFR vectors show a prevailing SW flow, GLOBAL vectors seem to represent a predominant southward flow near the coast.

References:

Berta, M., Bellomo, L., Magaldi, M. G., Griffa, A., Molcard, A., Marmain, J., Borghini, M., and Taillandier, V.: Estimating Lagrangian transport blending drifters with HF radar data and models: Results from the TOSCA experiment in the Ligurian Current (North Western Mediterranean Sea), Prog. Oceanogr., 128, 15–29, https://doi.org/10.1016/j.pocean.2014.08.004, 2014.

Aguiar, E., Mourre, B., Juza, M., Reyes, E., Hernández-Lasheras, J., Cutolo, E., Mason, E., and Tintoré, J.: Multi-platform model assessment in the Western Mediterranean Sea: impact of downscaling on the surface circulation and mesoscale activity, Ocean Dnam., 70, 273–288, https://doi.org/10.1007/s10236-019-01317- 8, 2020.

Lorente, P., Sotillo, M. G., Amo-Baladrón, A., Aznar, R., Levier, B., Aouf, L., Dabrowski, T., Pascual, Á. De, Reffray, G., Dalphinet, A., Toledano, C., Rainaud, R., and Álvarez-Fanjul, E.: The NARVAL Software Toolbox in Support of Ocean Models Skill Assessment at Regional and Coastal Scales, in ICCS 2019, Lecture Notes in Computer Science, edited by: Rodrigues, J., (Cham: Springer), https://doi.org/10.1007/978-3-030-22747- 0_25, 2019.

Lorente, P., Lin-Ye, J., García-León, M., Reyes, E., Fernandes, M., Sotillo, M. G., Espino, M., Ruiz, M. I., Gracia, V., Perez, S., Aznar, R., Alonso-Martirena, A., and Álvarez-Fanjul, E.: On the Performance of High Frequency Radar in the Western Mediterranean During the Record-Breaking Storm Gloria, Front. Mar. Sci., 8, 205, https://doi.org/10.3389/fmars.2021.645762, 2021.

5) For the upwelling event #2 (Figure 3c), the HFR data around latitude 41.4ºN show a localized drop of intensity of the CUI-HFR which is not consistent with the model (Figure 3d) The same phenomenon is visible for the upwelling event #1 although less pronounced (Figure 3a). At first sight this could be interpreted as a systematic error of the HFR measurement in this area. On the other hand, the Chlorophyll map on Figure 1a) shows the same disconnected structures around the same latitude, supporting the HFR pattern. Could you comment on this qualitative difference between HFR and GLOBAL in this case?

This dipole-like structure has already been observed in the CUI-HFR maps for July 2014 and reported by Lorente et al. (2020) in the same area. Furthermore, both cores were also evidenced in satellite-derived SST and CHL maps (Figure 8a in Lorente et al., 2020), in agreement with the spatial distribution of CUI-HFR.

The discrepancies detected between both CUI-HFR and CUI-GLOBAL maps in this specific subregion could be attributed, to a large extent, to the inherent shortcomings of a global ocean model, among others:

i) The coarse model spatial resolution (1/12º = 9.25 km), which handicaps the detection of smaller (sub)mesoscale features.

ii) The underestimation (or even the misrepresentation) of some coastal processes that could play a secondary role in the surface coastal circulation, like the freshwater discharge from Galician rivers (coincident with the upper core of cold SST, higher CHL and higher CUI-HFR). GLOBAL model includes only the impact of 100 major rivers by means of a smoothed climatology (Product User Manual, 2022)

It is also worth mentioning that the dipole-like structure has been observed several times at different relative positions, highlighting: i) the importance of the Galician shoreline orientation (with respect to the prevailing wind direction) in modulating upwelling features; ii) the importance of Cape Finisterre promontory. Abrupt changes in coastal orientation can induce noticeable wind stress fluctuations and, hence, different upwelling conditions with subsequent biophysical implications, as previously documented by Álvarez et al. (2005 and 2011) and Torres et al. (2003) in the same region.

A paragraph has been added to the manuscript to better clarify this point.

References:

Lorente, P., Piedracoba, S., Montero, P., Sotillo, M. G., Ruiz, M. I. and Álvarez-Fanjul, E.: Comparative Analysis of Summer Upwelling and Downwelling Events in NW Spain: A Model-Observations Approach, Remote Sens., 12(17), doi:10.3390/rs12172762, 2020.

Product User Manual (November 2022):

https://catalogue.marine.copernicus.eu/documents/PUM/CMEMS-GLO-PUM-001-024.pdf

Álvarez, I.; Gómez-Gesteira, M.; deCastro, M.; Prego, R. Variation in upwelling intensity along the North-West Iberian Peninsula (Galicia). J. Atmos. Ocean Sci. 2005, 10, 309–324.

Álvarez, I.; Gómez-Gesteira, M.; deCastro, M.; Lorenzo, M.N.; Crespo, A.J.C.; Dias, J.M. Comparative analysis of upwelling influence between the western and northern coast of the Iberian Peninsula. Cont. Shelf Res. 2011, 31, 388–399.

Torres, R.; Barton, E.D.; Miller, P.; Álvarez-Fanjul, E. Spatial patterns of wind and sea surface temperature in the Galician upwelling region. J. Geophys. Res. 2003, 108, 3130.

What can be said on the reliability of HFR measurement around this small area?

To ensure the consistency and reliability of HFR remote sensed estimations, an integrated approach was adopted, which consisted of: i) the real-time web monitoring of non velocity-based diagnostic parameters along with ii) regular-scheduled validation exercises of HFR data (at both the radial and total vector levels) against independent *in situ* observations in order to provide upper bounds on the radar current measurement accuracy.

Regarding the first point, we have a dedicated internal website to operationally monitor radar system health in real time (Lorente et al., 2016). This automated quality control application analyses a variety of diagnose parameters (SNR3, etc.), considered as indicators of possible malfunctions or abnormal status, to evaluate site performance. Abrupt or gradual degradation and failure problems can be easily detected, triggering alerts for troubleshooting. The alert algorithm, based on a ternary flag system, has been implemented to detect anomalies and categorize them in order to create a historic database of flagged radial files for a later offline reprocessing when one (or more) HFR site status is (are) considered to be working abnormally. According to this tool, the radar sites overall performance and their day-to-day operation were robust and within tolerance ranges during the analysed period. Furthermore, GDOP values remained below the imposed threshold (as defined in the methodology section) in order to screen out the less reliable data.

Regarding the second point, both eulerian and lagrangian validation exercises were conducted during 2021-2022 within the frame of RADAR ON RAIA project, an Interreg España-Portugal (POCTEP) programme. HFR-derived hourly surface currents were compared against Silleiro fixed buoy (denoted in Figure 1a) and drifter buoys measurements. Results revealed a good agreement for both components (correlation in the ranges 0.53-0.74), in accordance with results previously reported in the literature (Cosoli et al., 2010; Kaplan et al., 2005). RMSE was higher for the meridional component than for the zonal one: 9.86 versus 7.65 $cm \cdot s^{-1}$.

In addition, for the Bay of Biscay HFR it can be highlighted some of the previous work where the radar data has already been used in combination with other observations to study surface coastal transport processes and showed good agreement (Rubio et al., 2011 and 2018; Solabarrieta et al., 2016, Manso-Narvarte et al. 2018 and 2021).

References:

Cosoli, S., Mazzoldi, A. and Gacic, M. Validation of surface current measurements in the Northern Adriatic Sea from High Frequency radars, Journal of Atmospheric and Oceanic Technology, Vol. 27, pages 908-919, 2010.

Kaplan, D.M., Largier, J. and Botsford, L.W. HF radar observations of surface circulation off Bodega Bay (northern California, USA). Journal of Geophysical Research, Vol. 110, C10020, pages 1-25, 2005.

Lorente, P., Piedracoba S., Soto-Navarro, J., Ruiz M.I., Alvarez-Fanjul E. and Montero, P. The High Frequency coastal radar network operated by Puertos del Estado (Spain): roadmap to a fully operational implementation. IEEE Journal of Oceanic Engineering, doi: 10.1109/JOE.2016.2539438, pages 1-17, May 2016.

Manso-Narvarte, I.; Rubio, A.; Jordà, G.; Carpenter, J.; Merckelbach, L.; Caballero, A. Three-Dimensional Characterization of a Coastal Mode-Water Eddy from Multiplatform Observations and a Data Reconstruction Method. Remote Sens. 2021, 13, 674. https://doi.org/10.3390/rs13040674

Manso-Narvarte, I., Caballero, A., Rubio, A., Dufau, C., and Birol, F.: Joint analysis of coastal altimetry and high-frequency (HF) radar data: observability of seasonal and mesoscale ocean dynamics in the Bay of Biscay, Ocean Sci., 14, 1265–1281, https://doi.org/10.5194/os-14-1265-2018, 2018.

Rubio A, Reverdin G, Fontán, A., González, M., Mader, J., 2011. Mapping near-inertial variability in the SE Bay of Biscay from HF radar data and two offshore moored buoys. Geophys. Res. Lett., 38 (19): L19607.

Rubio A, Solabarrieta L, González M, Mader J, Castanedo S, Medina R, Charria G., Aranda J.A., 2013. Surface circulation and Lagrangian transport in the SE Bay of Biscay from HF radar data. OCEANS - Bergen, 2013 MTS/IEEE, doi: 10.1109/OCEANS-Bergen.2013.6608039

Rubio, A., Caballero, A., Orfila, A., Hernández-Carrasco, I., Ferrer, L., González, M., Solabarrieta, L., Mader, J., 2018. Remote Sensing of Environment, 205, 290-304, doi: 10.1016/j.rse.2017.10.037

Solabarrieta, L., Frolov, S., Cook, M., Paduan,J., Rubio, A., González,M., Mader, J., Charria, G., 2016. Skill assessment of HF radar-derived products for lagrangian simulations in the Bay of Biscay. J. Atmos. Oceanic Technol., 33, 2585–2597, doi: 10.1175/JTECH-D-16-0045.1.

6) page 9 line 280: «with» respect to
Done!